Vol 15 No 2, February 2006
1009-1963/2006/15(02)/0444-05

Chinese Physics

© 2006 Chin. Phys. Soc.
and IOP Publishing Ltd

Deposition and characterization of $YBCO/CeO_2/YSZ/CeO_2$ multilayers on biaxially textured Ni substrates*

Wang Shu-Fang(王淑芳)[a)†], Zhao Song-Qing(赵嵩卿)[b)], Liu Zhen(刘 震)[b)], Zhou Yue-Liang(周岳亮)[b)], Chen Zheng-Hao(陈正豪)[b)], Lü Hui-Bin(吕惠宾)[b)], Jin Kui-Juan(金奎娟)[b)], Cheng Bo-Lin(程波林)[b)], and Yang Guo-Zhen(杨国桢)[b)]

[b)] *Physics and Technology College of Hebei University, Baoding* 071002, *China*

[b)] *Laboratory of Optical Physics, Institute of Physics and Center of Condensed Matter Physics, Chinese Academy of Sciences, Beijing* 100080, *China*

(Received 5 July 2005; revised manuscript received 31 October 2005)

$CeO_2/YSZ/CeO_2$ buffer layers were deposited on biaxially textured Ni substrates by pulsed laser deposition. The influence of the processing parameters on the texture development of the seed layer CeO_2 was investigated. Epitaxial films of YBCO were then grown *in situ* on the CeO_2/YSZ (yttria-stabilized ZrO_2)/CeO_2-buffered Ni substrates. The resulting YBCO conductors exhibited self-field critical current density J_c of more than 1 MA/cm^2 at 77K and superconducting transition temperature T_c of about 91K.

Keywords: YBCO films, buffer layers, pulsed laser deposition, biaxially textured Ni substrates
PACC: 7475, 7470V, 8115I, 7460J

1. Introduction

New approaches leading to the possibility of fabricating biaxially textured YBCO on metallic substrates are currently under development in many laboratories around the world.[1–3] The rolling-assisted biaxially textured substrates (RABiTS) approach has been regarded as one of the leading techniques for fabrication of YBCO-coated conductors.[4–6] The main requirement in RABiTS technology is the deposition of one or more buffer layers on the biaxial texture of the metal substrate. These buffer layers are employed to transfer the substrate texture to the YBCO films as well as to prevent metal diffusion into the superconductors from the substrates. Primary considerations for these buffer layers must include proper matching of the adjacent crystalline lattices and thermal expansion coefficients, as well as chemical compatibility and easy deposition.

A successful RABiTS buffer layer structure is CeO_2/YSZ (yttria-stabilized ZrO_2)/CeO_2.[7,8] In this triple-layer structure, the CeO_2 seed layer can effectively minimize the formation of NiO during the initial deposition on the substrate, while the CeO_2 cap layer provides good lattice matching for the subsequent YBCO layer.[9] The intermediate YSZ layer serves as an oxygen and metal diffusion barrier. The CeO_2 cap layer on YSZ also provides chemical compatibility by suppressing the growth of $BaZrO_3$ which may occur at the YSZ/YBCO interface, causing degraded critical currents in the YBCO.[10] As either seed or cap layer, the CeO_2 film must be quite thin or else cracks will develop in thicker films due to the lattice mismatch and thermal expansion mismatch with the substrates and the YBCO layers.

In this paper, we report the epitaxial growth of $CeO_2/YSZ/CeO_2$ buffer layers on biaxially textured Ni substrates using pulsed laser deposition (PLD). A study of the effect of the substrate temperature on texture development of CeO_2 seed layer is presented. Using this $CeO_2/YSZ/CeO_2$ architecture as the buffer layers, high-quality YBCO films with a T_c about 91 K

*Project supported by the State Key Development Program for Basic Research of China (Grant No 2006CB601005).
†E-mail: wsf@aphy.iphy.ac.cn

万方数据

and a self-field critical current density J_c over 10^6 A/cm^2 at 77 K can be obtained.

2. Experiment

Biaxially textured Ni (99.99%) substrates were prepared by a cold rolling and annealing process. The thickness of the biaxially textured Ni substrates used was about 200 μm. Both the buffer layer CeO_2/YSZ/CeO_2 and YBCO film were grown by PLD, using a 308 nm XeCl excimer laser system operated at an energy density of about 2 J/cm^2 and a repetition rate of 4 Hz. A CeO_2 ceramic target, a 10mol% YSZ ceramic target and a YBCO ceramic target were used to deposit the CeO_2, YSZ and YBCO layers, respectively. All layers in this work have been deposited *in situ* without breaking the vacuum conditions after the completion of every run.

After the vacuum in the chamber had reached 10^{-4}Pa at room temperature, a gas mixture of 4% H_2 and 96% Ar was introduced until the pressure inside the chamber reached 100 Pa. The Ni substrates were annealed at 650°C for 1–2h to reduce the NiO on the surface of Ni substrates. The chamber was then pumped and maintained at a pressure of 1 Pa using a gas mixture of 4% H_2 and 96% Ar. An epitaxial CeO_2 seed layer, ≈40 nm thick, was deposited by PLD on the Ni substrates at 300–800°C. After the deposition of the CeO_2 seed layer, an initial layer of 30 nm YSZ was deposited at 10^{-4} Pa of O_2 and 700°C, followed by the additional growth of a 400 nm thick YSZ film and a 30 nm thick CeO_2 film with P_{O_2}=0.5–1 Pa at the same temperature. After deposition of the final buffer layer, the oxygen pressure was subsequently increased to 70 Pa and the superconducting YBCO film with a thickness of 600 nm was then deposited on the buffer layer at 850°C. After deposition, the sample was annealed at 500°C for about 20min at an oxygen pressure slightly below 1 atm, and then the sample was cooled down to room temperature.

Crystalline structures of the buffer layers and YBCO film were characterized by x-ray diffraction (XRD) techniques with $\theta - 2\theta$ scan, φ-scan, ω-scan and pole figure. The resistance measurement was performed with a standard four-probe method. The self-field critical current density, J_c, was measured at 77 K using an inductive technique.

3. Results and discussion

3.1. CeO_2 seed layers on textured Ni substrates

It is found that the processing parameters such as deposition gas pressure and temperature have a great effect on the crystal structure of the CeO_2 seed layer. The degree of the c-axis preferred orientation of the CeO_2 is reduced at both low and high deposition gas pressure. Good c-axis orientation is obtained only for CeO_2 layers deposited in the deposition gas pressure range of 0.5–1.5 Pa.

In order to obtain the desired (00l) oriented CeO_2 layers, we kept the forming gas pressure at 1 Pa and then deposited CeO_2 layers at different temperatures. Figure 1 shows the typical XRD $\theta - 2\theta$ scans for CeO_2 seed layers deposited on the textured Ni substrates at different temperatures. As the temperature increases from 300 to 700°C, the intensity of the (111) oriented CeO_2 peak decreases and the pure (002) oriented growth is achieved at about 650°C. However, the CeO_2 (111) peak has been observed again if the temperature exceeds 700°C. Besides, as the deposition temperature increases, the position of the CeO_2 (002) peak shifts to the high angle side (shown in the inset of Fig.1), which means that the in-plane lattice constants of the CeO_2 layers increase with increasing deposition temperature. The reason may be that the linear coefficient of thermal expansion of Ni is bigger than that of CeO_2, resulting in less lattice mismatch and hence less in-plane contraction of the CeO_2 layers deposited at higher temperatures.[11]

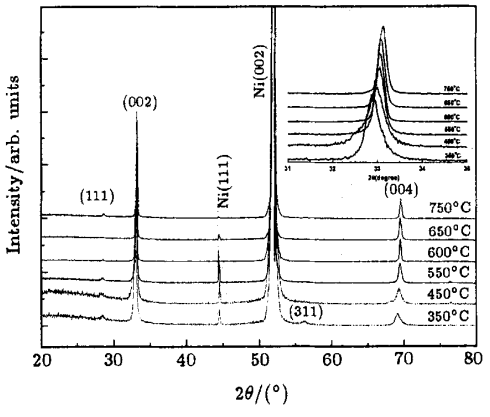


Fig.1. XRD $\theta - 2\theta$ scans for CeO_2 layers grown on textured Ni substrates at different temperatures. The inset is the $\theta - 2\theta$ scans for CeO_2 (002) peaks.

A typical $\theta - 2\theta$ scan for a 40 nm thick CeO_2 layer grown on the textured Ni substrate under the optimal experimental condition, i.e. T_s=650°C and P=1 Pa, is shown in Fig.2. The CeO_2 layer has a preferred c-axis orientation and no NiO exists in the

万方数据

layer. The inset of Fig.2 shows the CeO_2 (111) x-ray pole figure. Four well-defined CeO_2 (111) poles are evenly distributed, which reveals the presence of single four-fold cube texture. In addition to the excellent crystalline quality, the SEM image of this 40 nm thick CeO_2 layer shows that the layer is smooth, uniform, crack-free and dense.

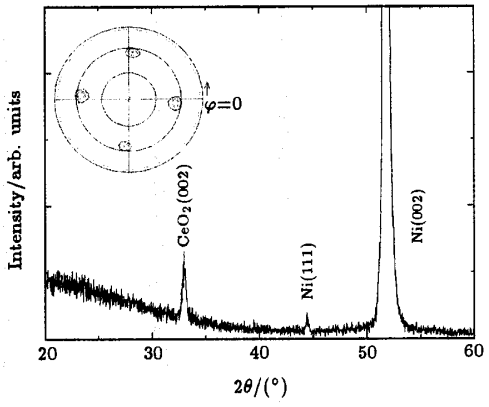


Fig.2. XRD $\theta - 2\theta$ scan for a 40 nm thick CeO_2 layer grown on textured Ni substrates at 650 °C and 1 Pa. The inset is the CeO_2 (111) x-ray pole figure of this CeO_2 layer.

3.2. CeO_2/YSZ buffer layers on CeO_2/Ni substrates

The growth conditions for the second and third buffer layers are not so critical as the seed layer. In all the experiments we could observe that the orientation of the seed buffer layer had transferred to the covering layers.

Figure 3 shows a typical $\theta - 2\theta$ scan for the CeO_2/YSZ/CeO_2 buffer layers deposited on textured Ni substrate by PLD. Single-phased (002) orientation of the buffer layers can be seen and the strong CeO_2 (002) and YSZ (002) signals reveal the presence of a good out-of-plane texture in both layers.

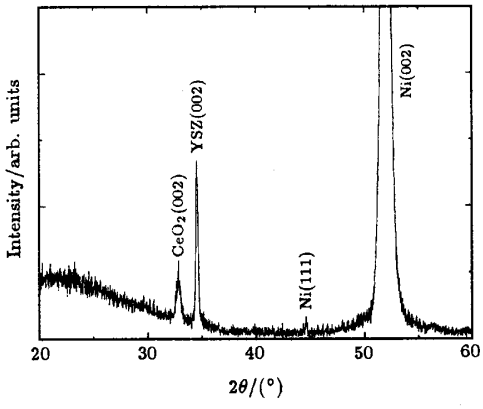


Fig.3. XRD $\theta - 2\theta$ scan for the CeO_2/YSZ/CeO_2/Ni structure.

Figure 4 shows ω-scan and φ-scan patterns for the CeO_2/YSZ/CeO_2/Ni structure. The full-width at half maximum (FWHM) of the φ-scan is usually used to quantitatively characterize the in-plane texture of the films and the out-of-plane texture of the films was characterized from that of ω-scans. It can be seen from the ω-scans that the out-of-plane texture is sharp, with FWHMs of the Ni (002), CeO_2 (002) and YSZ (002) being 7.0, 5.5 and 4.4, respectively. There is a significant improvement in the out-of-plane texture. This could be due to the formation of sub-grains inside the Ni grains, and also the smoothness of the CeO_2 and YSZ layers.[12] In the case of in-plane texture, the FWHMs of Ni (111), CeO_2 (111) and YSZ (111) are found to be 10.6, 11.1 and 9.9, respectively. Unlike the out-of-plane texture, no systematic improvement in the in-plane texture has been found. The XRD results from ω and φ scans indicate the existence of excellent epitaxy throughout all layers.

万方数据

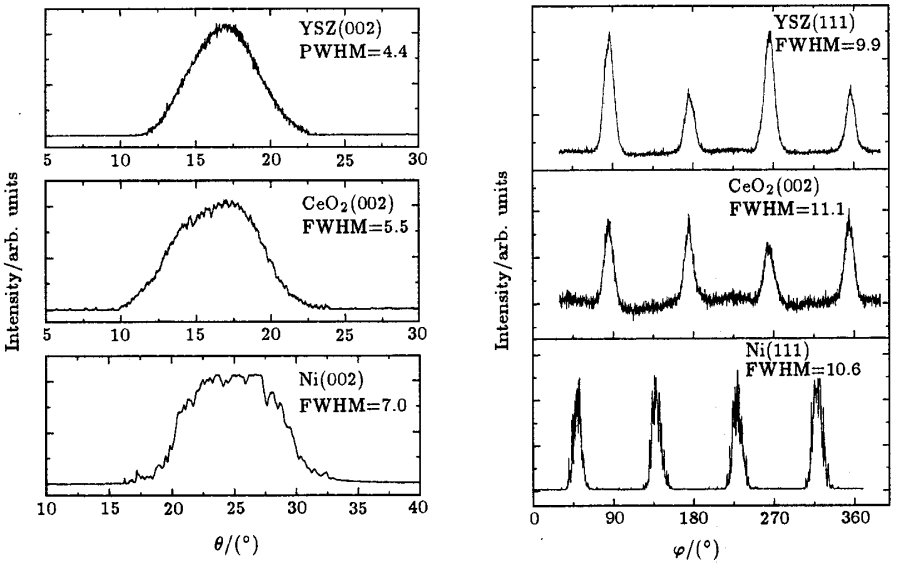


Fig.4. ω-scan and φ-scan patterns for the CeO_2/YSZ/CeO_2/Ni structure.

The Ni (111), CeO_2 (111) and YSZ (111) pole figures confirm that CeO_2 and YSZ buffer layers are biaxially textured, and there is a 45° rotation between the in-plane CeO_2/YSZ axes and Ni axes, indicating a cube-on-diagonal epitaxy with the epitaxial relationship of YSZ [110]//CeO_2[110]//Ni[100], as shown in Fig.5.

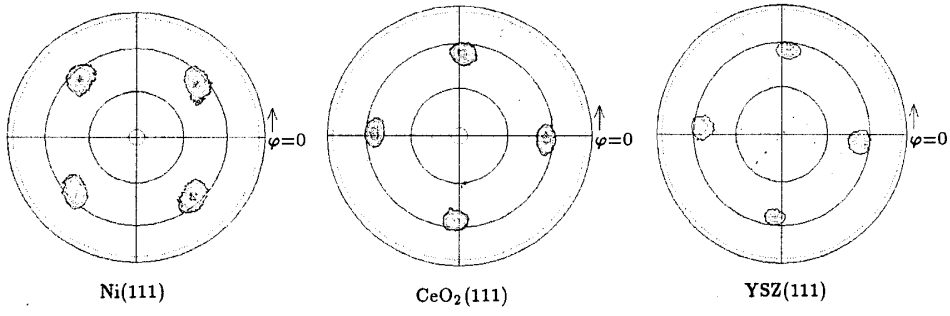


Fig.5. Pole figures of Ni (111), CeO_2(111) and YSZ (111) for the CeO_2/YSZ/CeO_2/Ni structure.

3.3. YBCO films on CeO_2/YSZ/CeO_2/Ni substrates

Highly textured PLD-YBCO has been grown on the CeO_2/YSZ/CeO_2 buffered Ni substrate. A typical $\theta - 2\theta$ scan for a 600 nm thick PLD-YBCO film on CeO_2/YSZ/CeO_2/Ni is shown in Fig.6, with the inset showing the YBCO (103) pole figure of the same YBCO film. The presence of only (00l) reflections indicates that the YBCO is c-axis oriented, and the pole figure reveals the presence of in-plane-texture. Detailed XRD results from ω-scans of YBCO (005) and φ-scan of YBCO (103) of the YBCO film reveal good biaxial texturing.

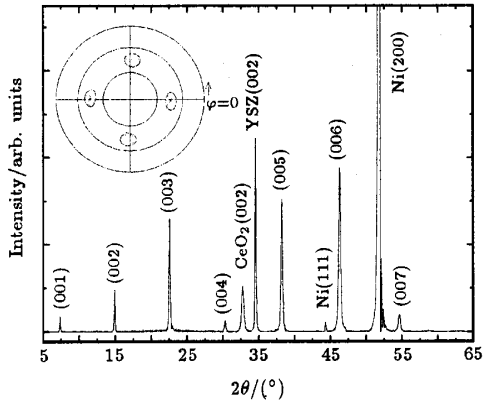


Fig.6. XRD $\theta - 2\theta$ scan for the YBCO film grown on CeO_2/YSZ/CeO_2/Ni structure. The inset is the YBCO (103) x-ray pole figure of this YBCO film.

万方数据

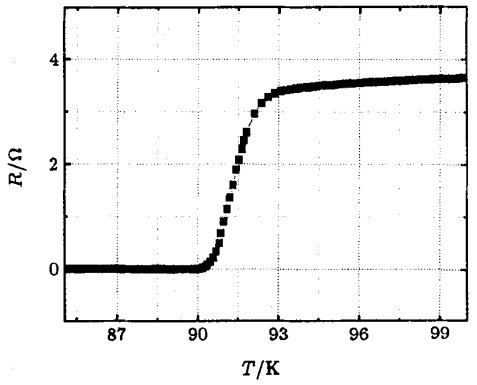


Fig.7. *R–T* curve for the YBCO film grown on the $CeO_2/YSZ/CeO_2/Ni$ structure.

We have obtained a T_c about 91 K for this 600 nm thick YBCO film, as shown in Fig.7. The critical current density J_c of the YBCO coated conductors was measured inductively, and average values of 1.4 MA/cm^2 can be obtained at 77 K in the self-field.

4. Conclusion

We have demonstrated the successful fabrication of high-quality epitaxial YBCO coatings on biaxially textured Ni substrates with a buffer layer sequence of $CeO_2/YSZ/CeO_2$. XRD measurements revealed good-quality crystalline structure for both buffer layers and YBCO films. The resulting YBCO coated conductors show a high T_c of 91 K and a self-field J_c of more than $1MA/cm^2$.

References

[1] Uprety K K, Ma B, Koritala R E, Fisher B L, Dorris S E and Balachandran U 2005 *Supercond. Sci. Technol.* **18** 294

[2] Worz B, Heinrich A and Stritzker D 2005 *Physica* C **418** 107

[3] Paranthaman M, Aytug T, Christen D K, Arendt P N, Foltyn S R, Groves J R, Stan L, Depaula R F, Wang H and Holesinger T G 2003 *J. Mater. Res.* **18** 2055

[4] Goyal A, Norton D P, Budai J D, Paranthaman M, Specht E D, Kroeger D M, Christen D K, He Q, Saffian B, List F A, Lee D F, Martin P M, Klabunde C E, Hartfield C E and Sikka V K 1996 *Appl. Phys. Lett.* **69** 1795

[5] Norton D P, Goyal A, Budai J D, Christen D K, Kroeger D M, Specht E D, He Q, Saffian B, Paranthaman M, Klabunde C E, Lee D F, Sales B C and List F A 1996 *Science* **274** 755

[6] Tomov B I, Kursumovic A, Majoros M, Kang D J, Glowacki B A and Evetts J E 2002 *Supercond. Sci. Technol.* **15** 598

[7] Chen J, Parilla P A, Bhattacharya R N and Ren Z F 2004 *Jpn. J. Appl. Phys.* **43** 6040

[8] Mathis J E, Goyal A, Lee D F, List F A, Paranthaman M, Christen D K, Specht E D, Kroeger D M and Martin P M 1998 *Jpn. J. Appl. Phys.* **37** L1379

[9] Barnes P N, Nekkanti R M, Haugan T J, Campbell T A, Yust N A and Evans J M 2004 *Supercond. Sci. Technol.* **17** 957

[10] Liu Z, Wang S F, Zhou Y L and Zhao S Q 2005 *Acta Phys. Sin.* **54** 2005 (in Chinese)

[11] Wang R P, Zhou Y L, Pan S H and Guo Z Y 1998 *J. Appl. Phys.* **84** 1994

[12] Paranthaman M, Aytug T, Zhai H Y, Heatherly L, Goyal A and Christen D K 2005 *Supercond. Sci. Technol.* **18** 223

万方数据